Scaling up a sign-ordered Kitaev chain without magnetic flux control

Liu, C.; Miles, Sebastian; Bordin, Alberto; Ten Haaf, Sebastiaan L.D.; Mazur, Grzegorz P.; Bozkurt, A. Mert; Wimmer, Michael

DOI
10.1103/PhysRevResearch.7.L012045

Publication date
2025

Document Version
Final published version

Published in
Physical Review Research

Letter

Scaling up a sign-ordered Kitaev chain without magnetic flux control

Chun-Xiao Liu,* Sebastian Miles, Alberto Bordin, Sebastiaan L. D. ten Haaf, Grzegorz P. Mazur, A. Mert Bozkurt, and Michael Wimmer
QuTech and Kavli Institute of Nanoscience, Delft University of Technology, Delft 2600 GA, The Netherlands

(Received 27 July 2024; accepted 17 January 2025; published 27 February 2025)

Quantum-dot-superconductor arrays have emerged as a new and promising material platform for realizing topological Kitaev chains. So far, experiments have implemented a two-site chain with limited protection. Here, we propose an experimentally feasible protocol for scaling up the chain in order to enhance the protection of the Majorana zero modes. To this end, we make use of the fact that the relative sign of normal and superconducting hoppings mediated by an Andreev bound state can be changed by electrostatic gates. In this way, our method only relies on the use of individual electrostatic gates on hybrid regions, quantum dots, and tunnel barriers, respectively, without the need for individual magnetic flux control, greatly simplifying the device design. Our work provides guidance for realizing a topologically protected Kitaev chain, which is the building block of error-resilient topological quantum computation.

DOI: 10.1103/PhysRevResearch.7.L012045

Introduction. The Kitaev chain is a paradigm of topological superconductivity that can host Majorana zero modes [1–15]. These zero-energy excitations are non-Abelian anyons which can be utilized to implement topological quantum computation [16,17]. Recently, quantum-dot-superconductor arrays have emerged as a promising platform for realizing a Kitaev chain [18]. A minimal two-site version [19] has been successfully realized in low-dimensional semiconductors, supported by tunnel spectroscopic evidence of Majorana zero modes at a fine-tuned sweet spot [20–22]. Crucially, a balance of the normal and superconducting coupling strengths is achieved by electrostatic gating on the hybrid region [23,24]. However, these finely tuned zero modes remain vulnerable to environmental noises due to a limited protection [19,23,25–31], which can be enhanced and become topological only after the quantum dot array is scaled up [1,18,32–35]. Furthermore, the experiments of anyonic fusion and braiding [36–39] to detect the non-Abelian statistics would not be possible before the Kitaev chain is extended to four or more sites.

In an extended chain ($N \geqslant 3$), the phases of the couplings become particularly important. In the limit of confinement to a one-dimensional channel as in experiments [20–22,40,41] and in the presence of a Rashba spin-orbit interaction and an axial magnetic field, an approximate complex conjugate symmetry [42] further constrains the effective couplings to be real numbers [18,43,44]. Thus, the problem of phase uncertainty is now reduced to *sign* uncertainty. For an N-site Kitaev chain

$$H_K = \sum_{n=1}^{N} \varepsilon_n f_n^\dagger f_n + \sum_{n=1}^{N-1} (t_n f_{n+1}^\dagger f_n + \Delta_n f_{n+1}^\dagger f_n^\dagger + \text{H.c.}), \quad (1)$$

the sweet-spot condition becomes

$$\varepsilon_n = 0, \quad |t_n| = |\Delta_n|, \quad \text{sgn}(t_1\Delta_1) = \text{sgn}(t_n\Delta_n), \quad (2)$$

where f_n is the annihilation operator of a spinless fermion, ε_n is the on-site energy, and t_n and Δ_n are the amplitudes of normal and superconducting tunnelings, respectively. In Ref. [18], the proposed solution to the sign problem was to use an individual magnetic flux control of the phase between neighboring superconducting grains. However, this would inevitably introduce multiple flux bias lines, thus complicating the device design and causing heating problems [see Fig. 1(a)]. In particular, the crosstalk of flux bias lines becomes an issue when using small superconducting loops, while larger-size loops would significantly increase the device size and thus limit the possible number of quantum dots to scale up.

In this Letter, we propose a scale-up protocol, where the sign problem is fixed purely in an electrostatic way *without* magnetic flux control [see Fig. 1(b)]. The physical insight here is that the two sweet spots mediated by an Andreev bound state (ABS) have opposite signs and can be explicitly detected in a three-site setup by conductance spectroscopy. Since a set of electrostatic gates is always needed to individually control ε_n, $|t_n|$, and $|\Delta_n|$ in a Kitaev chain, our proposal does not introduce any additional overhead in the device fabrication. Instead, our method greatly simplifies the device design and makes the platform suitable for implementing scalable topological quantum computation.

Sign of sweet spot. We first consider a minimal setup consisting of double quantum dots connected by a hybrid

*Contact author: chunxiaoliu62@gmail.com

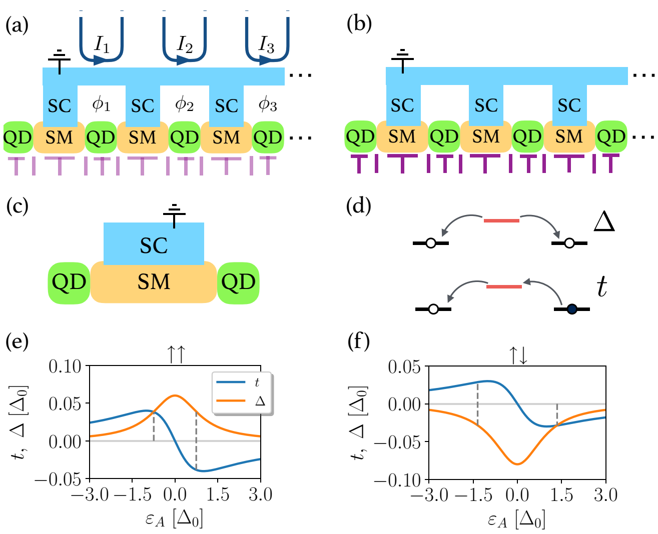

FIG. 1. (a) Schematic of a device with magnetic flux control using bias lines. (b) Schematic of a device where the phase difference is controlled purely by electrostatic gates (purple lines). (c) and (d) Schematic of a two-site Kitaev chain and the virtual processes that induce effective couplings of Δ and t. (e) and (f) Dependence of the coupling amplitudes on the chemical potential of the Andreev bound states.

segment. The Hamiltonian is [23–26,45]

$$\begin{aligned}
H &= H_{D,1} + H_{A,1} + H_{D,2} + H_{DAD,1},\\
H_{D,i} &= \sum_{\sigma=\uparrow,\downarrow} (\varepsilon_{Di} + \sigma E_{Zi}) n_{Di\sigma} + U_{Di} n_{Di\uparrow} n_{Di\downarrow},\\
H_{A,i} &= \sum_{\sigma=\uparrow,\downarrow} \varepsilon_{Ai} n_{Ai\sigma} + (\Delta_i c_{Ai\uparrow} c_{Ai\downarrow} + \text{H.c.}),\\
H_{DAD,i} &= \sum_{\sigma=\uparrow,\downarrow} \big(t_{\text{sc},i} c^\dagger_{Ai\sigma} c_{Di\sigma} + t'_{\text{sc},i} c^\dagger_{Di+1\sigma} c_{Ai\sigma}\\
&\quad + \sigma t_{\text{sf},i} c^\dagger_{Ai\bar\sigma} c_{Di\sigma} + \sigma t'_{\text{sf},i} c^\dagger_{Di+1\bar\sigma} c_{Ai\sigma} + \text{H.c.}\big).
\end{aligned} \tag{3}$$

Here, H_D is the Hamiltonian for a quantum dot, ε_D is the orbital energy, E_Z is the induced Zeeman spin splitting, and U_D is the Coulomb repulsion. H_A is the Hamiltonian of a subgap ABS in the hybrid region, ε_A is the normal-state energy, and Δ is the induced pairing. H_{DAD} describes single-electron tunneling between dots and hybrids, and t_{sc} (t_{sf}) is the amplitude for spin-conserving (spin-flipping) processes. When the direction of the spin-orbit field is perpendicular to the applied magnetic field [40,41], t_{sc}, t_{sf} are real [18,42]. Here, we assume a single dot orbital and single ABS in H_D and H_A, respectively. This approximation is accurate when the level spacings are large, i.e., $\Delta\varepsilon_D > E_Z$ and $\Delta\varepsilon_A > t_{\text{sc}}, t_{\text{sf}}$, as discussed in Ref. [23] and demonstrated in recent experiments [22,24].

In the tunneling regime where $|t_{\text{sc}}|, |t_{\text{sf}}| \ll \Delta, E_Z$, the effective couplings can be obtained using perturbation theory,

$$\begin{aligned}
t_{\uparrow\uparrow} &= (t_{\text{sf},1} t'_{\text{sf},1} - t_{\text{sc},1} t'_{\text{sc},1}) \frac{u^2 - v^2}{E_A},\\
\Delta_{\uparrow\uparrow} &= (t_{\text{sc},1} t'_{\text{sf},1} + t_{\text{sf},1} t'_{\text{sc},1}) \frac{2uv}{E_A},
\end{aligned} \tag{4}$$

where $t_{\uparrow\uparrow}$ and $\Delta_{\uparrow\uparrow}$ are the effective normal and superconducting couplings between spin-up orbitals in two quantum dots. $u^2 = 1 - v^2 = 1/2 + \varepsilon_A/2E_A$ are the coherence factors, and $E_A = \sqrt{\varepsilon_A^2 + |\Delta_0|^2}$ is the excitation energy. Figure 1(e) shows the dependence of $t_{\uparrow\uparrow}$ and $\Delta_{\uparrow\uparrow}$ on the chemical potential of the hybrid region, with model parameters $\Delta_1 = \Delta_0$, $t_{\text{sc}} = 3t_{\text{sf}} = 0.3\Delta_0$. Here, both amplitudes are real due to complex conjugate symmetry [42], and, furthermore, the two sweet spots have opposites signs, i.e.,

$$\begin{aligned}
t_{\uparrow\uparrow} &= \Delta_{\uparrow\uparrow}, \qquad \text{for } \varepsilon_A = -\varepsilon_A^*,\\
t_{\uparrow\uparrow} &= -\,\Delta_{\uparrow\uparrow}, \quad \text{for } \varepsilon_A = \varepsilon_A^*,
\end{aligned} \tag{5}$$

where $\varepsilon_A^* = \Delta_0 (t_{\text{sc},1} t'_{\text{sf},1} + t_{\text{sf},1} t'_{\text{sc},1})/(t_{\text{sf},1} t'_{\text{sf},1} - t_{\text{sc},1} t'_{\text{sc},1}) = 0.75\Delta_0$. We emphasize that the existence of two opposite-sign sweet spots is a robust feature as evidenced in Eq. (4). For example, when the strength of the spin-orbit interaction becomes much stronger ($3t_{\text{sc}} = t_{\text{sf}} = 0.3\Delta_0$), the only effect is that $t_{\uparrow\uparrow}$ obtains an overall minus sign, thus only reversing the signs of the sweet spots relative to Fig. 1(e). In addition, change of the parity of the bound-state wave functions ($t \to -t$ or $t' \to -t'$) would only give a common minus sign to both $t_{\uparrow\uparrow}$ and $\Delta_{\uparrow\uparrow}$, not affecting the sweet-spot properties either. On the other hand, the coupling amplitudes between orbitals of opposite spins are

$$\begin{aligned}
t_{\uparrow\downarrow} &= -(t_{\text{sc},1} t'_{\text{sf},1} + t_{\text{sf},1} t'_{\text{sc},1}) \frac{u^2 - v^2}{E_A},\\
\Delta_{\uparrow\downarrow} &= (t_{\text{sf},1} t'_{\text{sf},1} - t_{\text{sc},1} t'_{\text{sc},1}) \frac{2uv}{E_A}.
\end{aligned} \tag{6}$$

Figure 1(f) shows the $t_{\uparrow\downarrow}$ and $\Delta_{\uparrow\downarrow}$ curves using the same model parameters as in Fig. 1(e). Now two sweet spots appear at $\varepsilon_A = \pm\varepsilon_A^*$ with $\varepsilon_A^* = \Delta_0 (t_{\text{sf},1} t'_{\text{sf},1} - t_{\text{sc},1} t'_{\text{sc},1})/(t_{\text{sc},1} t'_{\text{sf},1} + t_{\text{sf},1} t'_{\text{sc},1}) = 4\Delta_0/3$, and, interestingly, their signs are reversed relative to the same-spin scenario. Here, in obtaining Eqs. (5) and (6), we have assumed no Zeeman splitting in ABS, which in general is expected to be reduced due to g-factor renormalization [46,47]. Nevertheless, even when this assumption is relaxed, it is still possible to find two opposite-sign sweet spots due to continuity [23,48]. Hence, we find that generically the relative sign of the normal and superconducting couplings can be changed by either changing the chemical potential in the hybrid region to switch to the other sweet spot or by changing the dot energy to switch the spin polarization, with both ways using electrostatic gating only.

Detection of π-phase shift. To experimentally detect the subtle sign of sweet spots, the minimal setup is a three-quantum-dot device with a superconducting loop connecting the two hybrid regions [see Fig. 2(a)]. Tunnel spectroscopy would distinguish the signs of the sweet spots by a π-phase shift. To support the statement, we now perform numerical calculations using the following Hamiltonian,

$$H = H_{D1} + H_{A1} + H_{D2} + H_{A2} + H_{D3} + H_{DAD,1} + H_{DAD,2}, \tag{7}$$

which includes three normal quantum dots connected by two ABSs. The Hamiltonians for dots, ABSs, and electron tunneling are almost identical to those in Eq. (3), except that now for H_A a phase difference determined by the

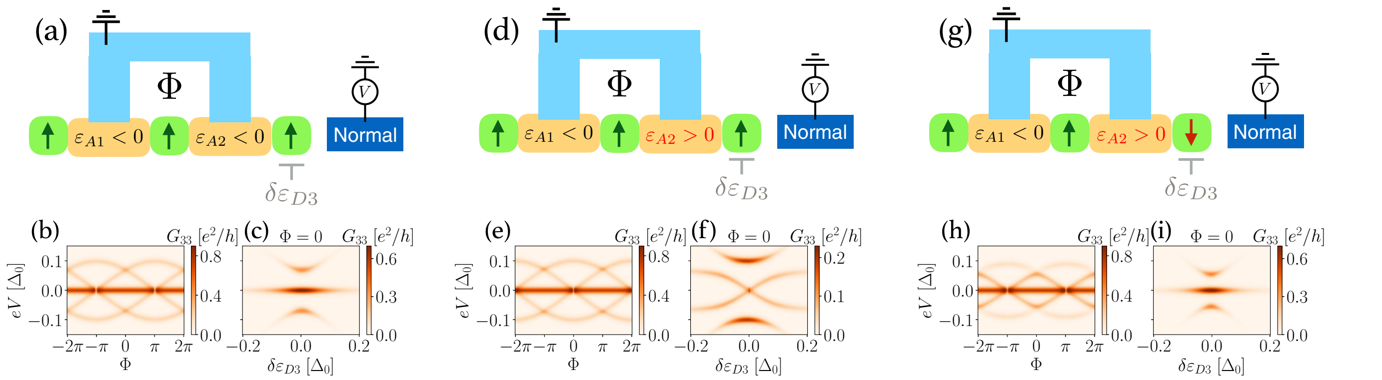

FIG. 2. Upper panels: Schematics of the transport setup to detect the signs of the sweet spots. Lower panels: Conductance spectroscopy ($G_{33} = dI_3/dV_3$) as a function of the magnetic flux or dot detuning. The systems in (a) and (g) are sign-ordered Kitaev chains at $\Phi = 0$, while in (d) the two sweet spots have opposite signs.

magnetic flux is included in the pairing potential, i.e., $\Delta_1 = \Delta_0$, $\Delta_2 = \Delta_0 e^{i\Phi}$. In addition, a normal-metal lead is tunnel coupled to dot $D3$, and conductance is numerically calculated using the rate-equation method [49,50].

We first consider a scenario where the two sweet spots are of the same type. By setting all three quantum dots to be spin up, this condition is satisfied when $\varepsilon_{A1} = \varepsilon_{A2} \approx -0.804\Delta_0$, which is close to the values predicted in Eq. (5). Figure 2(b) shows that a sign-ordered three-site Kitaev chain indeed appears at $\Phi = 0$ with a stable and isolated zero-bias conductance peak induced by Majorana zero modes. Additionally, this zero-bias peak is robust against detuning of dot $D3$ [see Fig. 2(c)], verifying that Majoranas are spatially localized.

When we change $\varepsilon_{A2} \approx 0.704\Delta_0$ while keeping ε_{A1} unchanged, the sign of the sweet spot mediated by $A2$ becomes opposite to $A1$ [see Fig. 1(e)]. As shown in Fig. 2(e), an additional zero-energy state appears in the vicinity of $\Phi = 0$, making the system gapless [37]. Unlike the sign-ordered chain, now the zero-bias peak is readily split with detuning of $D3$ [see Fig. 2(f)] due to the hybridization between the Majorana and the additional zero-energy state see Supplemental Material [48]. Moreover, by comparing Figs. 2(b) and 2(e) the sign switch of the sweet spot is clearly revealed as a π-phase shift in the flux-dependent conductance spectroscopy.

In the third scenario, we flip the spin of $D3$ into spin-down, which can be experimentally implemented by electrostatic gating. The chemical potential of $A2$ is still positive: $\varepsilon_{A2} \approx 1.3\Delta_0$. Indeed, Figs. 2(h) and 2(i) show the emergence of a sign-ordered Kitaev chain again, confirming the predictions made in Fig. 1(f). Therefore, flipping the spin of the dot orbitals provides an additional knob for correcting the sign of sweet spots.

Protocol for scaling up. Based on the findings in the previous sections, we now put forward our protocol for scaling up a long sign-ordered Kitaev chain. To this end, we require an experimental setup that can (i) be used to tune two neighboring dots to a sweet spot, for example, as discussed in Refs. [20–22,26], and (ii) detect whether the zero-energy degeneracy splits when the energy of the final dot is detuned from the resonance. In general, this requires that the superconducting leads that proximitize different hybrid regions form a single grounded lead. The two measurements can be realized for example by coupling each normal dot to an individual normal lead, forming a multiterminal junction. Alternatively, it is also sufficient to only contact the final dot with a normal lead, as shown in Fig. 2 or using gate sensing. Our protocol allows to build up the chain iteratively dot by dot.

Step 0. To begin with, we assume that we have already obtained a sign-ordered N-site Kitaev chain ($N \geqslant 2$) as shown in Fig. 3(a) (for $N = 2$, this corresponds to finding the sweet spot). Our goal is to extend it to $N + 1$ sites by choosing an appropriate sweet spot for the newly added dot.

Step 1. First, we focus on a two-site system formed by the Nth and $N + 1$th quantum dots decoupled from the rest of the array [see the dashed rectangle in Fig. 3(b)]. This can be achieved by closing the tunnel barriers outside the two dots, or, alternatively, by shifting all the other dots off resonance, as illustrated in the experiments of Refs. [34,35]. Then by electrostatic gating on the hybrid region, a sweet spot with $|t_N| = |\Delta_N|$ can be reached, e.g., signified by a cross in the charge stability diagram [see Fig. 3(b)] [20–22]. However, the sign of the sweet spot remains uncertain so far.

Step 2. We then form a three-site chain by coupling the $N - 1$th, Nth, and $N + 1$th dots, e.g., by lowering tunnel barriers or by bringing the $N - 1$th dot back to resonance [see Fig. 3(c)]. We measure the conductance spectroscopy against the detuning of dot-$N + 1$ [see Fig. 3(c)]. If the zero-bias peak is robust, we have successfully extended an N-site chain to $N + 1$ and can continue with the next dot. Otherwise, we have to return to step 1 to tune to the other sweet spot or the other dot spin, effectively flipping the relative sign between t_N and Δ_N.

Effect of phase fluctuations. In a realistic device, complex conjugate symmetry can be broken due to a finite width of the one-dimensional channel, the magnetic orbital effect on the dot or ABS wave functions, or a misaligned magnetic field. After performing a gauge transformation, an N-site chain ($N \geqslant 3$) can have $N - 2$ independent phase fluctuations, i.e., $\Delta_i = |\Delta_i| e^{i\delta\phi_i}$ for $i = 2, 3, \ldots, N - 1$ see Supplemental Material [48]. Here, we focus on the energy gap in the presence of phase fluctuations, since $|t_i| = |\Delta_i|$ guarantees the presence

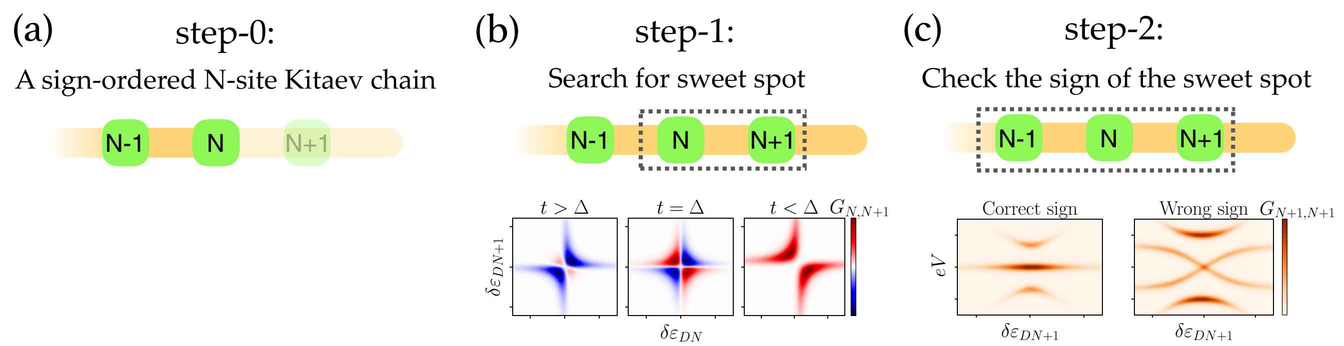

FIG. 3. Protocol for tuning up a sign-ordered Kitaev chain. (a) Preparation: Get ready a sign-ordered N-site chain ($N \geqslant 2$). (b) Step 1: Switch on the coupling between the Nth and $N+1$th dots while decoupling them from the rest of the system, e.g., by closing the tunnel barriers indicated by the vertical lines of the rectangle or by detuning all the other dot orbitals off resonance. Find the sweet spot $|t| = |\Delta|$ in the charge stability diagram. (c) Step 2: Connect the $N+1$th dot with the Nth and $N-1$th dots, and measure the differential conductance against the detuning of dot-$N+1$. If the zero-bias conductance peak remains robust, we thereby obtain a sign-ordered $N+1$-site Kitaev chain. Otherwise, we should return to step 1 to find a new sweet spot and test it in step 2 until success.

of a zero energy. Here, phase fluctuation obeys a uniform distribution of $\delta\phi_i \in [-\delta\phi, \delta\phi]$ for an ensemble of size 2000. As shown in Fig. 4, both the averaged and the minimal gap decrease monotonically with either the number of sites or the phase fluctuation amplitude. Interestingly, a longer chain is more prone to becoming gapless when $\delta\phi > \pi/2$. We hence expect that our protocol remains applicable even for small deviations from one dimensionality, as the sign of the sweet spot can still be used to minimize the phase difference. Put another way, reducing the cross-section area of the semiconducting nanowires would suppress the phase deviations induced by the magnetic orbital effects [47], thus optimizing the protection of Majorana zero modes.

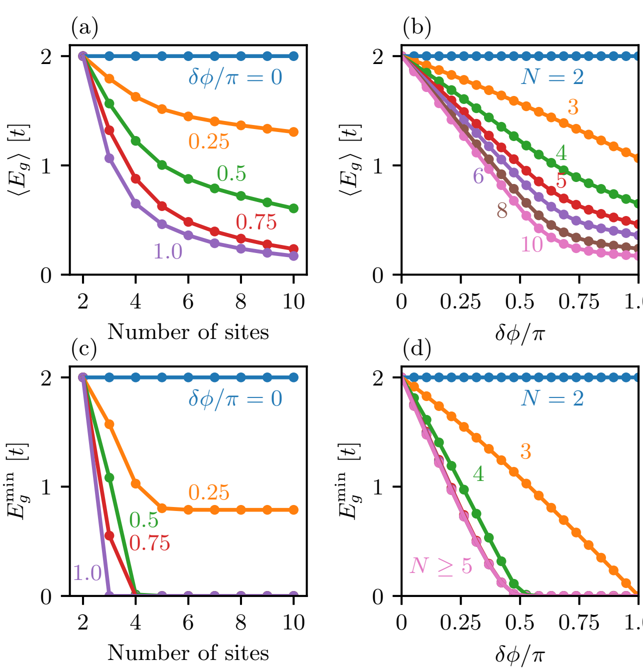

FIG. 4. (a) and (b) Mean of the excitation gap of a Kitaev chain vs the number of sites and phase fluctuation amplitude. (c) and (d) Minimal excitation gap vs the number of sites and phase fluctuation amplitude.

Discussion. In previous works, it was suggested to satisfy the phase-matching condition in an extended Kitaev chain by controlling the magnetic flux through a superconducting loop [18,51]. However, devices with small loops [see Fig. 1(a)] would suffer from crosstalk issues of the flux bias lines, while larger loops would significantly increase the system size by tens of micrometers, making it difficult to fit into a nanoscale device and limiting the number of dots to scale up. Within this context, our scale-up proposal uses a purely electrostatic method, thus eliminating the need for the cumbersome magnetic flux control. Most crucially, such a gate configuration is needed anyway to fine tune the sweet-spot values of $\varepsilon_n = 0$ and $|t_n| = |\Delta_n|$, so it does not add any fabrication overhead to the device design. Practically, the electrostatic gate configurations have already been implemented as a set of finger gates in recent experiments of three-site chains [34,35], which can be further generalized to longer chains. Therefore, we note the crucial difference between the upscaling protocol proposed in Ref. [51] and ours is that here we rely only on the electrostatic gates that are already present in the device. There is no need for additional gates or additional current lines for magnetic flux control.

Summary. In this Letter, we discover that the sweet spot mediated by ABS has a *sign* uncertainty, which was overlooked and undetectable in two-site chain studies [20–23,25–27,52–54], but will become crucial in an extended chain. Based on that, we give a concrete and practical protocol for scaling up a Kitaev chain using only electrostatic gates, eliminating the need for a magnetic flux control. It avoids the adverse heating issue and at the same time maintains a small nanoscale device size, both of which will benefit the eventual implementation of a scalable topological quantum computer. In particular, the gate configuration and control required in our proposal have been implemented in a recent experiment [35], adding to the practicality of our work. We thus believe that our proposal provides guidance to realizing a long topological Kitaev chain for implementing topological quantum computing [16,17] as well as demonstrating the non-Abelian statistics of Majorana anyons [36,38,39].

Acknowledgments. We are grateful to N. van Loo, F. Zatelli, and L. P. Kouwenhoven for useful discussions. This work was supported by a subsidy for top consortia for knowledge and innovation (TKI toeslag), by the Dutch Organization for Scientific Research (NWO) through OCENW.GROOT.2019.004, and by Microsoft Corporation Station Q.

C.-X.L. conceived the project idea and designed the project with input from A.B., S.L.D.t.H., G.P.M., and M.W.; C.-X.L. carried out the calculations with input from S.M. and A.M.B.; C.-X.L. and M.W. wrote the manuscript with input from all authors; C.-X.L. and M.W. supervised the project.

Data availability. The codes for generating the data and figures in the manuscript are available at Ref. [55].

[1] A. Y. Kitaev, Unpaired Majorana fermions in quantum wires, Phys. Usp. **44**, 131 (2001).
[2] J. Alicea, New directions in the pursuit of Majorana fermions in solid state systems, Rep. Prog. Phys. **75**, 076501 (2012).
[3] M. Leijnse and K. Flensberg, Introduction to topological superconductivity and Majorana fermions, Semicond. Sci. Technol. **27**, 124003 (2012).
[4] C. W. J. Beenakker, Search for Majorana fermions in superconductors, Annu. Rev. Condens. Matter Phys. **4**, 113 (2013).
[5] T. D. Stanescu and S. Tewari, Majorana fermions in semiconductor nanowires: Fundamentals, modeling, and experiment, J. Phys.: Condens. Matter **25**, 233201 (2013).
[6] J.-H. Jiang and S. Wu, Non-Abelian topological superconductors from topological semimetals and related systems under the superconducting proximity effect, J. Phys.: Condens. Matter **25**, 055701 (2013).
[7] S. R. Elliott and M. Franz, *Colloquium:* Majorana fermions in nuclear, particle, and solid-state physics, Rev. Mod. Phys. **87**, 137 (2015).
[8] M. Sato and S. Fujimoto, Majorana fermions and topology in superconductors, J. Phys. Soc. Jpn. **85**, 072001 (2016).
[9] M. Sato and Y. Ando, Topological superconductors: A review, Rep. Prog. Phys. **80**, 076501 (2017).
[10] R. Aguado, Majorana quasiparticles in condensed matter, Riv. Nuovo Cimento **40**, 523 (2017).
[11] R. M. Lutchyn, E. P. A. M. Bakkers, L. P. Kouwenhoven, P. Krogstrup, C. M. Marcus, and Y. Oreg, Majorana zero modes in superconductor–semiconductor heterostructures, Nat. Rev. Mater. **3**, 52 (2018).
[12] H. Zhang, D. E. Liu, M. Wimmer, and L. P. Kouwenhoven, Next steps of quantum transport in Majorana nanowire devices, Nat. Commun. **10**, 5128 (2019).
[13] E. Prada, P. San-Jose, M. W. A. de Moor, A. Geresdi, E. J. H. Lee, J. Klinovaja, D. Loss, J. Nygård, R. Aguado, and L. P. Kouwenhoven, From Andreev to Majorana bound states in hybrid superconductor–semiconductor nanowires, Nat. Rev. Phys. **2**, 575 (2020).
[14] S. M. Frolov, M. J. Manfra, and J. D. Sau, Topological superconductivity in hybrid devices, Nat. Phys. **16**, 718 (2020).
[15] K. Flensberg, F. von Oppen, and A. Stern, Engineered platforms for topological superconductivity and Majorana zero modes, Nat. Rev. Mater. **6**, 944 (2021).
[16] C. Nayak, S. H. Simon, A. Stern, M. Freedman, and S. Das Sarma, Non-Abelian anyons and topological quantum computation, Rev. Mod. Phys. **80**, 1083 (2008).
[17] S. D. Sarma, M. Freedman, and C. Nayak, Majorana zero modes and topological quantum computation, npj Quantum Inf. **1**, 15001 (2015).
[18] J. D. Sau and S. D. Sarma, Realizing a robust practical Majorana chain in a quantum-dot-superconductor linear array, Nat. Commun. **3**, 964 (2012).
[19] M. Leijnse and K. Flensberg, Parity qubits and poor man's Majorana bound states in double quantum dots, Phys. Rev. B **86**, 134528 (2012).
[20] T. Dvir, G. Wang, N. van Loo, C.-X. Liu, G. P. Mazur, A. Bordin, S. L. D. ten Haaf, J.-Y. Wang, D. van Driel, F. Zatelli, X. Li, F. K. Malinowski, S. Gazibegovic, G. Badawy, E. P. A. M. Bakkers, M. Wimmer, and L. P. Kouwenhoven, Realization of a minimal Kitaev chain in coupled quantum dots, Nature (London) **614**, 445 (2023).
[21] S. L. D. ten Haaf, Q. Wang, A. M. Bozkurt, C.-X. Liu, I. Kulesh, P. Kim, D. Xiao, C. Thomas, M. J. Manfra, T. Dvir, M. Wimmer, and S. Goswami, A two-site Kitaev chain in a two-dimensional electron gas, Nature (London) **630**, 329 (2024).
[22] F. Zatelli, D. van Driel, D. Xu, G. Wang, C.-X. Liu, A. Bordin, B. Roovers, G. P. Mazur, N. van Loo, J. C. Wolff, A. M. Bozkurt, G. Badawy, S. Gazibegovic, E. P. A. M. Bakkers, M. Wimmer, L. P. Kouwenhoven, and T. Dvir, Robust poor man's Majorana zero modes using Yu-Shiba-Rusinov states, Nat. Commun. **15**, 7933 (2024).
[23] C.-X. Liu, G. Wang, T. Dvir, and M. Wimmer, Tunable superconducting coupling of quantum dots via Andreev bound states in semiconductor-superconductor nanowires, Phys. Rev. Lett. **129**, 267701 (2022).
[24] A. Bordin, G. Wang, C.-X. Liu, S. L. D. ten Haaf, N. van Loo, G. P. Mazur, D. Xu, D. van Driel, F. Zatelli, S. Gazibegovic, G. Badawy, E. P. A. M. Bakkers, M. Wimmer, L. P. Kouwenhoven, and T. Dvir, Tunable crossed Andreev reflection and elastic cotunneling in hybrid nanowires, Phys. Rev. X **13**, 031031 (2023).
[25] A. Tsintzis, R. S. Souto, and M. Leijnse, Creating and detecting poor man's Majorana bound states in interacting quantum dots, Phys. Rev. B **106**, L201404 (2022).
[26] C.-X. Liu, A. M. Bozkurt, F. Zatelli, S. L. D. ten Haaf, T. Dvir, and M. Wimmer, Enhancing the excitation gap of a quantum-dot-based Kitaev chain, Commun. Phys. **7**, 235 (2024).
[27] R. S. Souto, A. Tsintzis, M. Leijnse, and J. Danon, Probing Majorana localization in minimal Kitaev chains through a quantum dot, Phys. Rev. Res. **5**, 043182 (2023).
[28] S. Miles, D. van Driel, M. Wimmer, and C.-X. Liu, Kitaev chain in an alternating quantum dot-Andreev bound state array, Phys. Rev. B **110**, 024520 (2024).
[29] J. D. T. Luna, A. M. Bozkurt, M. Wimmer, and C.-X. Liu, Flux-tunable Kitaev chain in a quantum dot array, SciPost Phys. Core **7**, 065 (2024).
[30] W. Samuelson, V. Svensson, and M. Leijnse, Minimal quantum dot based Kitaev chain with only local superconducting proximity effect, Phys. Rev. B **109**, 035415 (2024).

[31] R. S. Souto and R. Aguado, Subgap states in semiconductor-superconductor devices for quantum technologies: Andreev qubits and minimal Majorana chains, in *New Trends and Platforms for Quantum Technologies*, edited by R. Aguado, R. Citro, M. Lewenstein, and M. Stern, Lecture Notes in Physics Vol. 1025 (Springer, Cham, 2024), pp. 133–223.

[32] M. Ezawa, Even-odd effect on robustness of Majorana edge states in short Kitaev chains, Phys. Rev. B **109**, L161404 (2024).

[33] A. Bordin, X. Li, D. van Driel, J. C. Wolff, Q. Wang, S. L. D. ten Haaf, G. Wang, N. van Loo, L. P. Kouwenhoven, and T. Dvir, Crossed Andreev reflection and elastic cotunneling in three quantum dots coupled by superconductors, Phys. Rev. Lett. **132**, 056602 (2024).

[34] A. Bordin, C.-X. Liu, T. Dvir, F. Zatelli, S. L. D. ten Haaf, D. van Driel, G. Wang, N. van Loo, T. van Caekenberghe, J. C. Wolff *et al.*, Signatures of Majorana protection in a three-site Kitaev chain, arXiv:2402.19382.

[35] S. L. D. ten Haaf, Y. Zhang, Q. Wang, A. Bordin, C.-X. Liu, I. Kulesh, V. P. M. Sietses, C. G. Prosko, D. Xiao, C. Thomas *et al.*, Edge and bulk states in a three-site Kitaev chain, arXiv:2410.00658.

[36] C.-X. Liu, H. Pan, F. Setiawan, M. Wimmer, and J. D. Sau, Fusion protocol for Majorana modes in coupled quantum dots, Phys. Rev. B **108**, 085437 (2023).

[37] B. Pandey, S. Okamoto, and E. Dagotto, Nontrivial fusion of Majorana zero modes in interacting quantum-dot arrays, Phys. Rev. Res. **6**, 033314 (2024).

[38] P. Boross and A. Pályi, Braiding-based quantum control of a Majorana qubit built from quantum dots, Phys. Rev. B **109**, 125410 (2024).

[39] A. Tsintzis, R. S. Souto, K. Flensberg, J. Danon, and M. Leijnse, Majorana qubits and non-Abelian physics in quantum dot–based minimal Kitaev chains, PRX Quantum **5**, 010323 (2024).

[40] G. Wang, T. Dvir, G. P. Mazur, C.-X. Liu, N. van Loo, S. L. D. ten Haaf, A. Bordin, S. Gazibegovic, G. Badawy, E. P. A. M. Bakkers, M. Wimmer, and L. P. Kouwenhoven, Singlet and triplet Cooper pair splitting in hybrid superconducting nanowires, Nature (London) **612**, 448 (2022).

[41] Q. Wang, S. L. D. ten Haaf, I. Kulesh, D. Xiao, C. Thomas, M. J. Manfra, and S. Goswami, Triplet correlations in Cooper pair splitters realized in a two-dimensional electron gas, Nat. Commun. **14**, 4876 (2023).

[42] S. Tewari and J. D. Sau, Topological invariants for spin-orbit coupled superconductor nanowires, Phys. Rev. Lett. **109**, 150408 (2012).

[43] M. Scheid, İ. Adagideli, J. Nitta, and K. Richter, Anisotropic universal conductance fluctuations in disordered quantum wires with Rashba and Dresselhaus spin–orbit interaction and an applied in-plane magnetic field, Semicond. Sci. Technol. **24**, 064005 (2009).

[44] M. Diez, J. P. Dahlhaus, M. Wimmer, and C. W. J. Beenakker, Andreev reflection from a topological superconductor with chiral symmetry, Phys. Rev. B **86**, 094501 (2012).

[45] F. Domínguez and A. L. Yeyati, Quantum interference in a Cooper pair splitter: The three sites model, Physica E **75**, 322 (2016).

[46] T. D. Stanescu, J. D. Sau, R. M. Lutchyn, and S. Das Sarma, Proximity effect at the superconductor-topological insulator interface, Phys. Rev. B **81**, 241310(R) (2010).

[47] A. E. Antipov, A. Bargerbos, G. W. Winkler, B. Bauer, E. Rossi, and R. M. Lutchyn, Effects of gate-induced electric fields on semiconductor Majorana nanowires, Phys. Rev. X **8**, 031041 (2018).

[48] See Supplemental Material at http://link.aps.org/supplemental/10.1103/PhysRevResearch.7.L012045 for (1) model parameter values for numerical calculations, (2) gauge transformation of the Kitaev chain, (3) effect of finite Zeeman energy in the Andreev bound states, and (4) hybridization of Majorana modes at the π phase.

[49] C. W. J. Beenakker, Theory of Coulomb-blockade oscillations in the conductance of a quantum dot, Phys. Rev. B **44**, 1646 (1991).

[50] H. Bruus and K. Flensberg, *Many-Body Quantum Theory in Condensed Matter Physics: An Introduction* (Oxford University Press, Oxford, UK, 2004).

[51] I. C. Fulga, A. Haim, A. R. Akhmerov, and Y. Oreg, Adaptive tuning of Majorana fermions in a quantum dot chain, New J. Phys. **15**, 045020 (2013).

[52] Z.-H. Liu, C. Zeng, and H. Q. Xu, Coupling of quantum-dot states via elastic cotunneling and crossed Andreev reflection in a minimal Kitaev chain, Phys. Rev. B **110**, 115302 (2024).

[53] A. M. Bozkurt, S. Miles, S. L. D. ten Haaf, C.-X. Liu, F. Hassler, and M. Wimmer, Interaction-induced strong zero modes in short quantum dot chains with time-reversal symmetry, arXiv:2405.14940.

[54] D. van Driel, R. Koch, V. P. M. Sietses, S. L. D. ten Haaf, C.-X. Liu, F. Zatelli, B. Roovers, A. Bordin, N. van Loo, G. Wang *et al.*, Cross-platform autonomous control of minimal Kitaev chains, arXiv:2405.04596.

[55] https://zenodo.org/records/14808369.